Available online at www.sciencedirect.com

ScienceDirect

Materials Today: Proceedings 7 (2019) 744–753

materialstoday: PROCEEDINGS

www.materialstoday.com/proceedings

Nanotech Malaysia 2018

Properties of rapid thermal oxidized p-type germanium and its metal-oxide-semiconductor capacitor structure

Norani Ab Manaf, Abdul Manaf Hashim*

Malaysia-Japan International Institute of Technology, Universiti Teknologi Malaysia, Jalan Sultan Yahya Petra, 54100 Kuala Lumpur, Malaysia

Abstract

In this study, p-type Ge surface was oxidized using a rapid thermal technique at temperatures of 380ºC, 400ºC, 450ºC and 500ºC, and annealing time of 5 min, 10 min and 15 min in oxygen (O_2) with fixed flow rate of 1.0 *l*/min. It was found that the surface roughness of germanium oxide (GeO_x) decreases with the increase of oxidation temperature and time due to the uniform desorption of GeO_x. The samples oxidized at 450ºC and 500ºC show low surface roughness. Four different oxidation states, namely, Ge^{1+}, Ge^{2+}, Ge^{3+}, and Ge^{4+} were confirmed in the thermally oxidized Ge surface. The fractional composition of these oxide species is strongly depended on the oxidation temperature and time. The fabricated MOS ($Au/GeO_x/Ge$) capacitor using the samples oxidized at 450ºC and 500ºC show low leakage current due to thicker GeO_x layer produced by high oxidation rate at such temperatures. A sample oxidized at 450ºC was found to show acceptable capacitive behavior up to 500kHz while a sample of 500ºC up to 1MHz. The results seem to suggest that an innovative control of Ge oxidation is needed in order to realize a practical Ge MOSFET in near future.

Selection and peer-review under responsibility of the scientific committee of the Nanotech Malaysia 2018.

Keywords: Germanium; thermal oxidation; capacitor; MOSFET

1. Introduction

The scaling down of the silicon metal-oxide-semiconductor field effect transistor (Si-MOSFET) is inevitable in order to enhance the performance of ultra-large scale integrated circuits (ULSIs) [1]. Scaling down of Si-MOSFET seems to reach its limit due to several problems such as short channel effect and so forth [2]. Hence, a new material which has superb properties over than Si is needed to improve the performance of ULSI. Germanium (Ge) is the

* Corresponding author. Tel.: +603-2203-1517; fax: +603-2203-1266.
E-mail address: abdmanaf@utm.my

Selection and peer-review under responsibility of the scientific committee of the Nanotech Malaysia 2018.

most promising candidate because it possesses electron mobility of 2 times and hole mobility of 4 times higher than that of Si [3]. Furthermore, Ge has large density of states (DOS). With its large DOS in conduction band gives another advantage for achieving large drive current as compared to other III-V semiconductor materials [4]. However, it is still difficult to realize high performance Ge MOSFET due to the lack of suitable gate insulating layer. Several new solutions such as insertion of high k-dielectric material as a gate insulating layer has been proposed [5]. Unfortunately, a problem still arises due to the creation of high interface state density (D_{it}) resulting in low hole and electron mobility [5].

Germanium oxide (GeO_x) has been considered as a promising candidate not only due to its process simplicity but also it can give relatively good insulation characteristics and low D_{it} [6]. However, as reported in many articles, GeO_x is not stable due to its high desorption rate when being heat-treated at high temperature [7]. There are several methods that are commonly used to grow GeO_x such as thermal oxidation [8], ozone oxidation [9], plasma oxidation [10] and so on. Among these methods, low-cost thermal oxidation is considered as a promising technique to grow GeO_x layer since high quality of GeO_x/Ge interface can be realized. In this work, a GeO_x layer is formed on p-type Ge substrate by thermal oxidation in oxygen (O_2) gas using rapid thermal process. The morphology and compositional characteristics are investigated. A direct current measurement and frequency response of fabricated MOS capacitor structure are also carried out.

2. Experimental

p-type Ge (100) substrate with resistivity of ~13.5 Ωcm was used. Prior to an oxidation process, a Ge substrate was cleaned to remove native oxide and impurities on the surface. Here, the substrate was cleaned with traditional organic cleaning followed by an immersion in the 10% hydrochloric (HCl) acid solution for 5 min. After rinsing with de-ionized (DI) water, the substrate was immersed again in diluted hydrofluoric (HF) solution ($HF:H_2O$, 1:50) for another 5 min. Finally, the substrate was inserted immediately into the furnace system as shown in Fig. 1(a) after being rinsed in DI water and dried with nitrogen (N_2) blow. In this study, a rapid thermal oxidation (RTO) was applied. After the substrate was inserted in the furnace, N_2 gas was inserted for 15 min to create inert ambient. After that, the temperature of furnace was rapidly increased to 450ºC in N_2 ambient and kept for 15 min to ensure all particles and contamination on the substrates were removed out. After this process, the furnace was stopped and cooled down in N_2 ambient. Finally, the furnace was rapidly heated again in N_2 ambient from room temperature to the oxidation temperature.

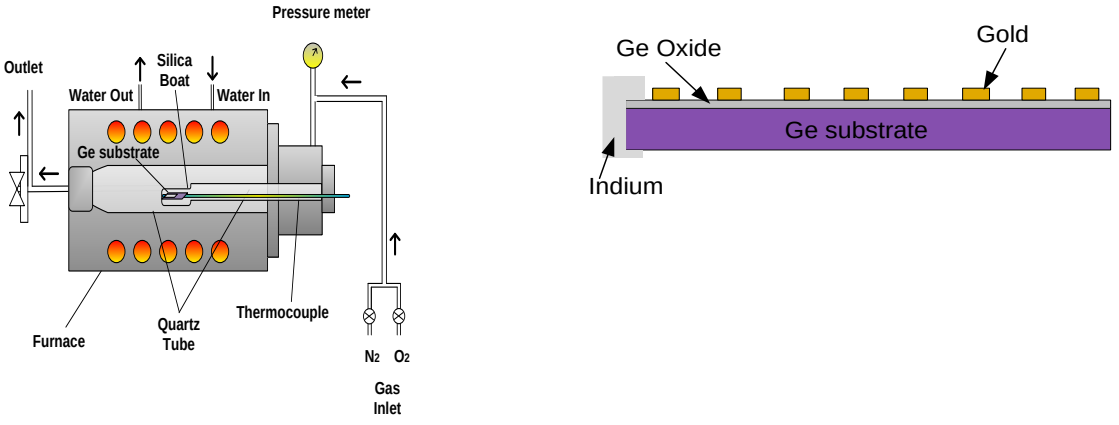

Fig. 1. (a) Experimental setup, (b) schematic of fabricated MOS structure.

After reaching the set oxidation temperature, N_2 flow was stopped and oxygen (O_2) with purity of 99.999% was introduced into the furnace. The oxidation times were done at 5 min, 10 min and 15 min, whereas oxidation temperatures were set at 380 °C, 400 °C, 450 °C and 500 ºC. After oxidation completed, both furnace and O_2 gas

were stopped and at the same time, N_2 gas was introduced again until the substrate temperature reached room temperature. A MOS capacitor structure as shown in Fig. 1(b) was fabricated by depositing gold (Au) on the front contact with diameter of 400 µm and thickness of 120 nm by using direct thermal evaporation through metal mask. The back contact was formed by indium (In). Here, the back contact was rubbed with sand paper and cleaned with ethanol to remove the native oxide layer before being placed onto the melted In and then, dried naturally. This was done in order to reduce the contact resistance at Au/Ge interface. In this study, atomic force microscopy (AFM) was used to measure the surface roughness of the GeO_x. X-ray photoelectron spectroscopy (XPS) was used to analyze the chemical state, stoichiometry and composition of oxide in GeO_x/Ge structure with Al kα source (1486.6 eV). Thickness of the GeO_x was measured by ellipsometry. Transmission electron microscopy (TEM) analysis was used to analyze the interface of GeO_x/Ge and to verify the thickness measured by ellipsometry. Current-voltage (I-V) measurement was performed using semiconductor parameter analyzer and capacitance-voltage (C-V) measurement was carried out using Keithley 4200 from 100 kHz to 1MHz.

3. Results and discussion

The effect of HF treatment on the surface roughness of Ge substrates was determined using AFM analysis. Fig. 2 shows the AFM topologies of Ge surface before and after HF treatment for 5 min. From a line scan analysis as depicted in Fig. 2, there was insignificant difference between both surfaces. The average of roughness was calculated from 6 scanned areas on each sample and was tabulated in Table 1.

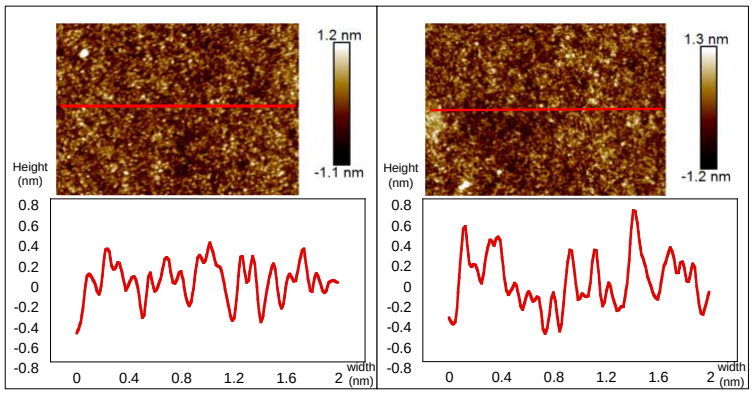

Fig. 2. AFM images of Ge surface (a) before HF treatment and (b) after HF treatment.

Table 1. Average of surface roughness of Ge surface before and after HF treatment.

Condition	Surface roughness (nm)						Average surface roughness (nm)
Before HF treatment	0.240	0.231	0.243	0.301	0.261	0.154	0.238
After HF treatment	0.243	0.245	0.247	0.311	0.298	0.289	0.272

It can be seen that the difference is very small for a such short etching time. However, it is worthy to note that longer etching time may cause the surface to be rough. To investigate the removal condition of native oxide from Ge surface after HF etching, XPS analysis was conducted. As shown in Fig. 3(a), there are two main peaks observed. The highest peak centered at binding energy of ~29.3 eV indicates the Ge 3d spectra of Ge element. Another peak centered at the binding energy of ~32.7 eV can be attributed to the native GeO_x. Meanwhile, as shown in Fig. 3(b), only a peak corresponds to Ge 3d of Ge element was observed without a peak of native GeO_x. This clearly indicates that native oxide was completely removed after HF treatment.

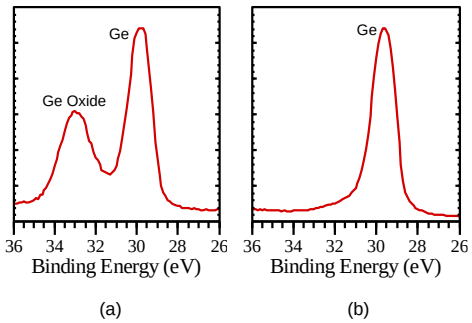

Fig. 3. XPS analysis of Ge surface (a) before HF treatment and (b) after HF treatment.

Fig. 4 summarizes the AFM topologies of thermally grown GeO_x at various oxidation temperatures and times. Surface roughness (RMS) values are determined from image areas of 2×2 μm^2.

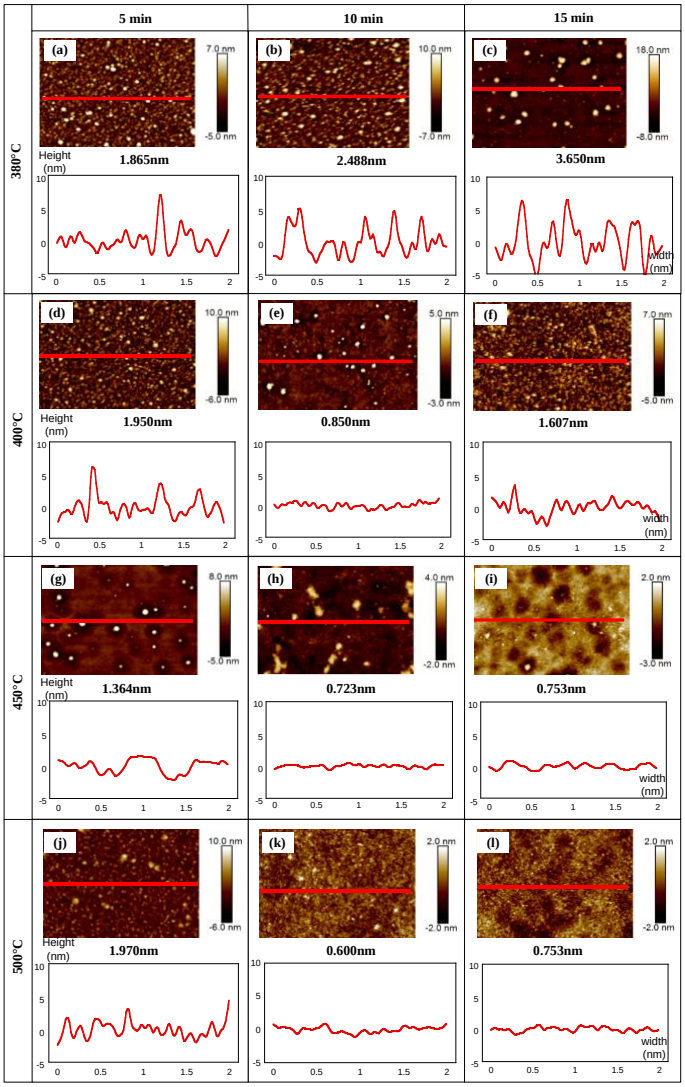

Fig. 4. AFM images of Ge surface after being oxidized at various temperatures and times.

From Fig. 4, several conclusions can be derived. The samples oxidized at 380 °C show extremely high surface roughness and it increases with the oxidation time. It is speculated that the desorption of GeO_x is not uniform. However, it shows a tendency of decrement of roughness with oxidation time for the samples oxidized at 450 °C and 500 °C, indicating uniform desorption. There is no significant change in the values of surface roughness for the samples oxidized for 5 min regardless of the oxidation temperatures. This is probably due to the oxidation time that is too short. It is also expected that the thickness of GeO_x layer increases with the oxidation temperature and time. For oxidation time of 5 min, it clearly shows that the difference of surface roughness is insignificant for all tested temperatures. The difference become larger for 10 min and 15 min of oxidation where it decreases with the increase of temperatures. Here, it can be also seen that the surface roughness increases almost linearly with time for the sample oxidized at 380 ºC speculated to be resulted from nonuniform desorption. Whereas, for the other temperatures, the surface roughness shows a slight decrement probably due to uniform desorption rate of GeO_x as indicated in Fig. 4.

As discussed in previous section, it is worth to briefly explain the mechanism of desorption of thermally oxidized Ge surface as well reported in literatures [8]. The mechanism of the GeO_x desorption is illustrated in Fig.5. During the oxidation process, Ge atom is consumed at the GeO_x/Ge interface [8]. It is considered that the interface reaction will not only promote generation of germanium dioxide (GeO_2) and germanium monoxide (GeO) but will simultaneously generate a loosely bonded Ge at interface by taking consideration of the backward reaction. This loosely bonded Ge will react with GeO_2 to create unstable or volatile GeO at the surface which will be desorbed or evaporated at high temperature. From Fig. 5, it can be said that both oxidation and desorption of sub-oxides happen simultaneously.

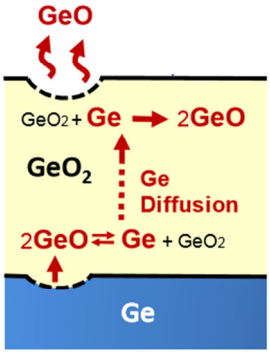

Fig. 5. Desorption mechanism of thermally oxidized Ge surface.

XPS analysis is conducted to investigate the dependence of oxidation temperature and time on the composition of oxide components. Fig. 6 shows the XPS analysis of oxides for the samples oxidized at 380 ºC, 400 ºC, 450 °C and 500 °C for 10 min in 1.0 *l*/min O_2. The deconvoluted XPS spectra reveal different oxidation states of Ge. The oxidation states Ge^{1+}, Ge^{2+}, Ge^{3+}, and Ge^{4+} as shown in Fig. 6 correspond to the oxide species of Ge_2O, GeO, Ge_2O_3, and GeO_2, respectively. Here, in this fitting, the peaks of Ge (elemental Ge $3d_{3/2}$, 29.8 eV), Ge^{1+} (Ge_2O $3d_{5/2}$, 30.6 eV), Ge^{2+} (GeO $3d_{5/2}$, 31.4 eV), Ge^{3+} (Ge_2O_3 $3d_{5/2}$, 32.4 eV), and Ge^{4+} (GeO_2 $3d_{5/2}$, 33.3 eV) were centered [11]. For the oxidation at 380ºC, the oxide peak consists of 4 different oxide components with oxidation state of Ge^{4+} that correspond to GeO_2 is significantly higher than the others. The intensity of sub-oxides decreases with the increase of temperatures. At temperature of 500ºC, the sub-oxide components almost disappear leaving only the sub-oxide of GeO_2. The disappearance of the other sub-oxide species from the surface may due to the aggressive desorption. To further understand the change in oxide composition with oxidation time, we perform XPS analysis of Ge 3d spectra for thermally oxidized Ge at temperature of 380 °C for 5 min, 10 min and 15 min. As shown in Fig. 7, the intensity of GeO_2 at 5 min (12) is smaller as compared to the intensity of GeO_2 at 15 min (18). This seems to indicate that the thickness of GeO_2 layer is thinner at 5 min.

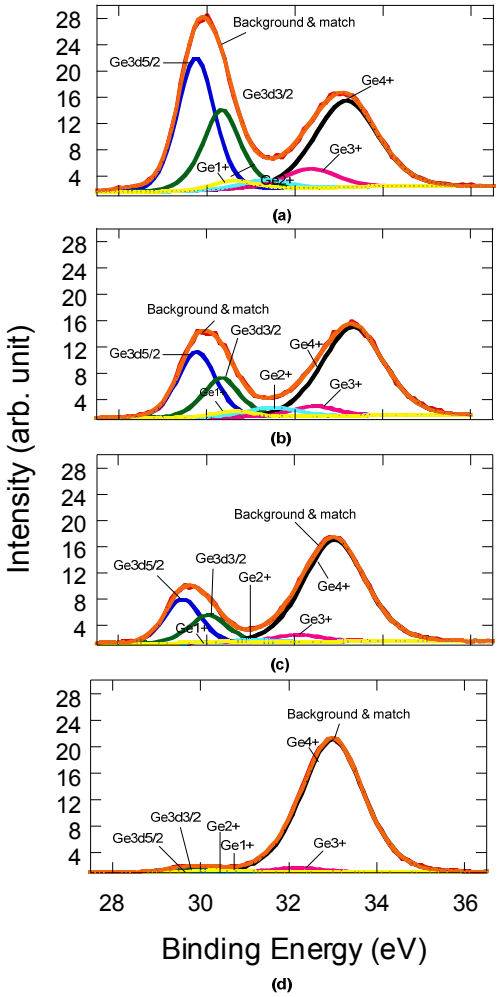

Fig. 6. XPS analysis of sub-oxides for samples oxidized at (a) 380°C, (b) 400°C, (c) 450°C, and (d) 500°C for 10 min.

Also, as shown in Fig. 7(a), the intensity of Ge substrate (32) is much higher than the intensity of GeO_2 peaks (12) which further justify a thin GeO_2 layer formed on Ge at low temperature of 380 °C. However, for a sample oxidized at 10 min and 15 min as shown in Fig. 7(b) and (c), respectively, the intensity of Ge substrate peak decreases, while the intensity of GeO_2 peak increases. This indicates that the thickness of GeO_2 layer increases with the oxidation times. However, the peaks correspond to the other sub-oxides are still observable due to low desorption of GeO_x at low temperature of 380 °C even though the desorption rate increases with the times, creating high surface roughness. Fig. 8 shows a cross-sectional TEM images for the thermally oxidized GeO_x fabricated at 500 ºC in 1.0 *l*/min O_2 for 10 min. It can be clearly seen that the interface is relatively smooth. The average thickness taken at 40 points is 7.525 nm. It worthy to mention that the average oxide thickness increases with the oxidation temperatures and it also shows drastic increment especially at temperature of 500 °C (data not shown). Fig. 9 shows the average thickness of thermally oxidized Ge at various temperatures and times measured by using ellipsometer. Here, the trend is in good agreement with the data given by TEM images. Again, the average oxide thickness increases with the oxidation temperatures where it shows a drastic increment especially at temperature of 500 °C.

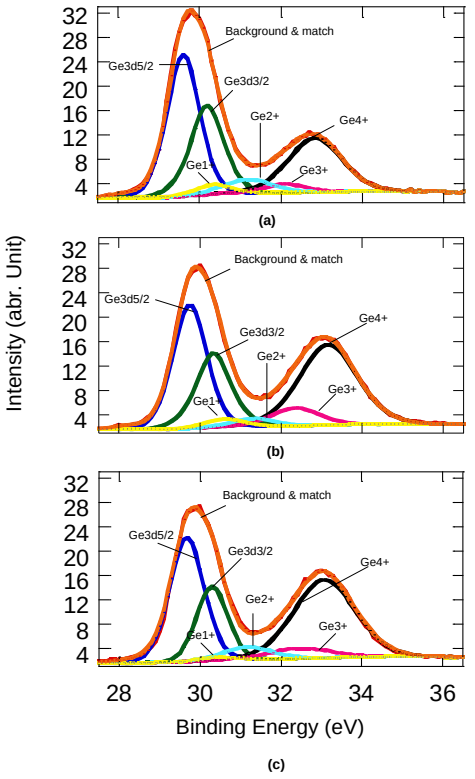

Fig. 7. XPS analysis of sub oxides for samples oxidized at 380°C for (a) 5 min, (b) 10 min, and (c) 15 min.

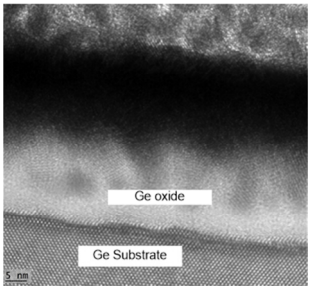

Fig. 8. TEM images of GeO_x/Ge interface.

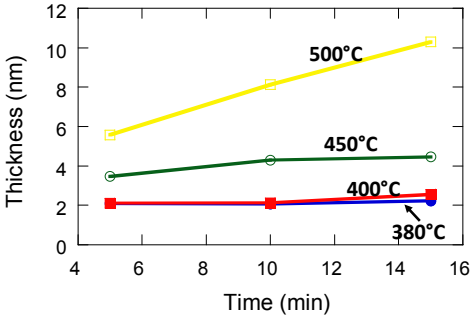

Fig. 9. Average thickness of Ge thermal oxide layer.

Fig. 10 shows the current-voltage (I-V) characteristics of the Au/GeO_x/Ge gate stack structures measured at room temperature for samples oxidized for 5 min, 10 min and 15 min at different oxidation temperatures in 1.0 *l*/min of O_2 flow. The scanned voltage is from -3V to 3V. As shown in Fig. 10, the same tendency has been observed where the leakage current decreases with the increase of the oxidation temperature for both forward and reverse biases. In particular, the samples oxidized at 380 ºC and 400 ºC show much higher leakage current as compared to samples oxidized at 450 ºC and 500 ºC. As shown in Fig. 9, the samples oxidized at 380 ºC and 400 ºC have thin and uneven thickness of GeO_x layer as compared to the samples oxidized at 450 ºC and 500 ºC. Generally, the current flow in MOS structure can be explained by two mechanisms. The first one is tunneling current which can be further divided to direct tunneling and Fowler-Nordheim (F-N) tunneling [12]. It is well reported that a direct tunneling will dominate when the oxide thickness is less than 4 nm, and F-N tunneling becomes dominant when the oxide thickness is in between 4-10 nm. The another one is a current resulted from the thermionic emission. Here, the thermionic or Schottky emission takes place when the electrons in the metal obtain enough energy provided by thermal activation, they will be able to overcome and tunnel through the energy barrier at the metal-dielectric interface.

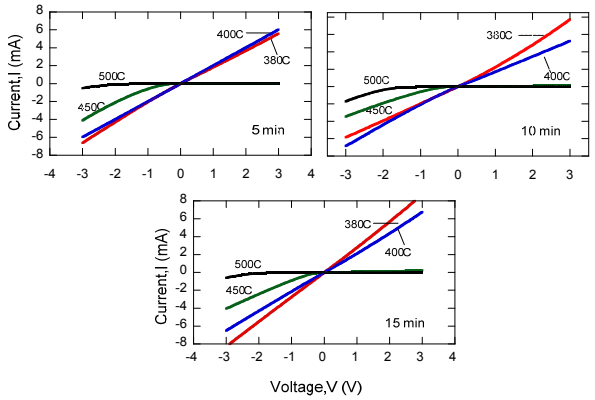

Fig. 10. I-V characteristics of Au/GeO_x/Ge stack structure.

Fig. 11 (a) and (b) shows log scale I-V characteristics of Au/GeO_x/Ge MOS structure oxidized at 450ºC and 500ºC in 1.0 *l*/min O_2, respectively as a function of oxidation times. As shown in Fig. 11, the leakage current decreases with the increase of oxidation times especially in the forward bias mode due to the formation of thicker oxide layer. In general, the capacitance properties of MOS devices is directly related to the quality of the dielectric material.

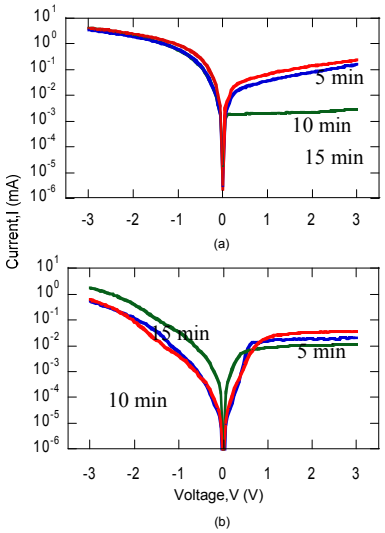

Fig. 11. I-V characteristics (log scale) of sample oxidized at (a) 450°C and (b) 500°C.

Fig. 12 shows a room temperature C-V measurement for Au/GeO_x/Ge MOS capacitors oxidized at 380ºC, 400ºC, 450ºC and 500ºC for 10 min. The measured frequency was set at 1 MHz. The oxide thickness for 380ºC, 400ºC, 450ºC and 500ºC samples were 2.074 nm, 2.134 nm, 4.308 nm and 8.136 nm, respectively. Here, the capacitance was measured under unidirectional gate bias sweep from negative to positive voltage. It can be observed that the capacitance in accumulation region for oxidized samples increases from 5 nF to 45 nF with oxidation temperatures. Samples oxidized at 380ºC and 400ºC show low capacitance in all regions, i.e. accumulation, depletion and inversion regions. As shown in Fig. 12, there was almost no capacitance in accumulation region for 380ºC and 400ºC oxidized samples. This is speculated that the thickness of the oxide is too thin and rough which may make it unable to generate capacitive behavior. On the other hand, as depicted in Fig. 12, the samples oxidized at 500ºC show acceptable C-V characteristics in those 3 regions. The flat band voltage (V_{FB}) shifted to the negative values. The negative shift in V_{FB} indicates that there are positive charges exist in the GeO_x/Ge oxide interface, existence of charges due to the holes trapped in the oxide layer or presence of positive ions in between the layer. This also well discussed in several reports [13].

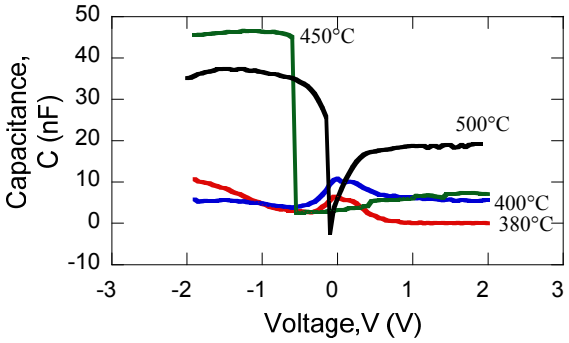

Fig. 12. C-V characteristics of Au/GeO_x/Ge MOS structure measured at 1 MHz.

The capacitance in accumulation region for sample 450ºC (45 nF) and 500ºC (35 nF) is slightly different due to a difference in thickness. As shown in Fig. 12, among those 4 samples, only a sample oxidized at 500ºC shows a capacitive characteristic in inversion region around 20 nF. This result indicates that GeO_x still can function as a dielectric film with acceptable property even at high frequency of 1 MHz. However, for sample 450ºC, there was no capacitance in inversion region when tested at such high frequency. To find the working frequency for sample 450ºC, C-V measurement was performed at low frequencies.

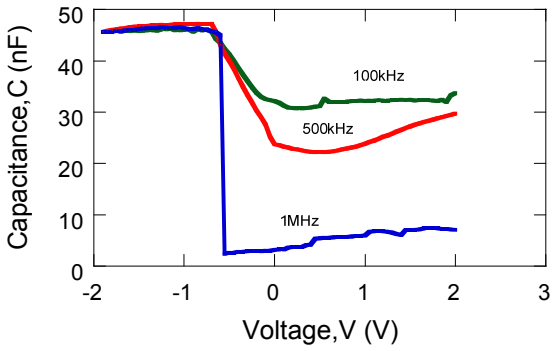

Fig. 13. C-V characteristics of Au/GeO_x/Ge MOS structure oxidized at 450°C.

Fig. 13 shows C-V characteristics for sample oxidized at 450ºC. At low frequencies of 100kHz and 500kHz, the depletion region is much wider than that of 1MHz, meaning that for both frequencies the sample behaves like capacitor. The sample has also shown frequency response in inversion region at 100kHz and 500kHz. Here, it can be said that the working frequency for sample 450ºC can be increased up to 500kHz.

4. Conclusion

In this study, p-type Ge surface was oxidized using a rapid thermal technique. It was found that the surface roughness of GeO_x decreases with the increase of oxidation temperature and time due to uniform desorption of GeO_x. 4 different oxidation states were confirmed in the thermally oxidized Ge surface. The fractional composition of these oxide species is strongly depended on the oxidation temperature and time. The fabricated MOS capacitor using the samples oxidized at 450ºC and 500ºC show low leakage currents due to high oxidation rate at such temperatures which increase the thickness of oxide layer. A sample oxidized at 450ºC was still able to show acceptable capacitance characteristics at frequency up to 500kHz while sample of 500ºC up to 1MHz.

Acknowledgements

N. A. M. thanks MARA and MOE for research scholarship. This work was funded by FRGS, MJIIT, Universiti Teknologi Malaysia, Malaysia Ministry of Science, Technology and Innovation, and the Malaysia Ministry of Education.

References

[1] G. E. Moore, Proceedings of the IEEE. 38 (1998) 82–85.
[2] C. C. Hu, Modern Semiconductor Devices for Integrated Circuits, 1st edition, Pearson, 2009.
[3] R. Zhang, N. Taoka, P. C. Huang, M. Takenaka, S. Takagi, in Proceedings of the International Electron Devices Meeting, Technical Digest (2011) 642–645.
[4] M. Takenaka, R. Zhang, S. Takagi, IEEE Int. Reliab. Phys. Symp. Proc. (2013) 1–8.
[5] L. Zhang, H. Li, Y. Guo, K. Tang, J. Woicik, J. Robertson, P. C. McIntyre, ACS Appl. Mater. Interfaces, 7 (2015) 20499–20506.
[6] S. N.A. Murad, P.T. Baine, D.W. McNeill, S.J.N. Mitchell, B. M. Armstrong, M. Modreanu, G. Hughes, R.K. Chellappan, Solid. State. Electron. 78 (2012) 136–140.
[7] K. Kita, C. H. Lee, T. Nishimura, K. Nagashio, A. Toriumi, in 215th ECS Meet (2009) 785.
[8] J. Oh, J. C. Campbell, Mater. Sci. Semicond. Process. 13 (2010) 185–188.
[9] D. Kuzum, T. Krishnamohan, A. J. Pethe, A. K. Okyay, Y. Oshima, Y. Sun, J. P. McVittie, P. a. Pianetta, P. C. McIntyre, K. C. Saraswat, IEEE Electron Device Lett. 29 (2008) 328–330.
[10] R. Zhang, X. Yu, M. Takenaka, S. Takagi, IEEE Trans. Electron Dev. 61 (2014) 2316–2323.
[11] N. Tabet, M. Salim, A. Al-Oteibi, J. Electron Spectros. Relat. Phenom.101 (1999) 233–238.
[12] C. Fu-Chien, Adv. Mater. Sci. Eng. 2014 (2014) 578168.
[13] Y. Zhou, M. Ogawa, X. Han, K. L. Wang, Appl. Phys. Lett. 93 (2008) 2012–2015.